Can Delhi's Pollution be Affected by Crop Fires in the Punjab Region?

Masayuki Takigawa[1], Prabir K. Patra[1], Yutaka Matsumi[2], Surendra K. Dhaka[3], Tomoki Nakayama[4], Kazuyo Yamaji[5], Mizuo Kajino[6], and Sachiko Hayashida[7]
[1]*Japan Agency for Marine-Earth Science and Technology, Yokohama, Japan*
[2]*Institute for Space-Earth Environmental Research, Nagoya University, Nagoya, Japan*
[3]*Radio and Atmospheric Physics Lab, Rajdhani College, University of Delhi, New Delhi, India*
[4]*Faculty of Environmental Science, Nagasaki University, Nagasaki, Japan*
[5]*Graduate School of Maritime Sciences, Kobe University, Kobe, Japan*
[6]*Meteorological Research Institute, Japan Meteorological Agency, Tsukuba, Japan*
[7]*Research Institute for Humanity and Nature, Kyoto, Japan*

Abstract

The severe air pollution events continue to occur every year during late October and early November in Delhi, forcing air/land traffic disruptions and anxiety in the daily life of the citizens. We analyze the behaviors of the air pollution events in October and November 2019 that arose from the crop-residue burning as seen using remote sensing techniques. Transport pathways and the mean transit time from the fire hotspots are evaluated using the FLEXPART (FLEXible PARTicle dispersion model). Our results suggest that the polluted regions in Delhi are partly influenced by the crop-residue burning. The uncertainty of our evaluation can be attributable to insufficient information on emission sources because the biomass burning emission based on daily-basis fire radiative power (FRP) of Moderate-Resolution Imaging Spectroradiometry (MODIS) is significantly degraded by the existence of hazy clouds. In future, it is desirable to establish a dense measurement network between Punjab and Delhi for the early detection of the source signals of aerosol emissions and their transport in this region. The FLEXPART model simulation shows the transport of emission signals from Punjab to Delhi, which further expands toward the Bengal region within a span of two days.

(**Citation**: Takigawa, M., P. K. Patra, Y. Matsumi, S. K. Dhaka, T. Nakayama, K. Yamaji, M. Kajino, and S. Hayashida, 2020: Can Delhi's pollution be affected by crop fires in the Punjab region? *SOLA*, **16**, 86−91, doi:10.2151/sola.2020-015.)

1. Introduction

Historically, air pollution and human health have been a major issue for the developing and fast-growing cities around the world, and Delhi has often topped the list of most polluted cities in the world (WHO 2016). The air pollution, especially caused by the particulate matter of aerodynamic diameter of 2.5 μm or less (PM2.5), is harmful to the human respiratory system (Balakrishnan et al. 2019). Aerosol emissions in India are dominated by transportation, industrial and residential energy usage and biomass burning (Guttikunda et al. 2014; Sharma et al. 2018; Saraswat et al. 2013).

Because of the extreme exposure to the PM2.5 in Delhi of large societal impact, number of studies have been conducted for understanding specific emission controls of Diwali festival and agricultural activities in the neighboring states during the late October to early November, and local infrastructural developments (Jethva et al. 2018; Kanawade et al. 2019; Mukherjee et al. 2018; Sawlani et al. 2019; Cusworth et al. 2018). High air pollution events are also linked with natural dynamical control, such as stagnation of airmass movement due to weak winds when the wind direction changed from southwesterly to northwesterly in the late October (Sawlani et al. 2019; Tiwari et al. 2013). It is also reported that the daily mortality caused by particle matters can be increased by 56% in the period of Diwali (Chen et al. 2020).

In this paper, we study the evolution and variabilities of PM2.5 in Delhi using data at a couple of sites. A Lagrangian transport model framework is employed to link the sources of black carbon (BC) emissions from agricultural waste burning to interstate pollution transport and beyond to the eastern part of the Indian subcontinent. The relationship between cloudiness and hotspot is analyzed using remote sensing data, and transport is diagnosed using the daily maps of the Aerosol Index, aided by the transit time of particles by the transport model.

2. Materials and methods

2.1 Surface and satellite observations

An observational site has been set up using a compact optical PM2.5 sensor (Panasonic-PM2.5 sensor) at Dwarka (28.58°N, 77.06°E) which is a sub-city of Delhi since May 2019. The sensor's performance was evaluated by year-round field observations in Japan (Nakayama et al. 2018). PM2.5 mass concentration observed at the US embassy in New Delhi (28.60°N, 77.19°E) was also used for the analysis (U.S. Embassy in India 2019). Hourly-basis observation was conducted at the US embassy using a beta attenuation monitor (MetOne BAM-1020) which is one of the measuring instruments certified by the US EPA (Environmental Protection Agency) (US EPA 2016). Both sites exist in the National Capital Region (NCR) of India, and the distance between these two sites is about 15 km. The geographical location of the target area is shown in Fig. 1. Locations of hotspots from FIRMS (Fire Information for Resource Management System) based on MODIS Collection 6 Active fire detections MCD14DL (NASA LANCE 2019) in October and November 2019 are also shown in Fig. 1. This period coincides well with the harvest season of rice in the states of Punjab and Haryana, India.

The offline version of the ultraviolet (UV) aerosol index (AI) of TROPOMI (Tropospheric Monitoring Instrument) on Sentinel-5 Precursor was also used for the analysis of the daily movement of pollutants' plume (Stein Zweers 2018). It offers daily-basis high-resolution (3.5×7 km^2) global distribution of column-amounted aerosols even in the presence of clouds. UVAI has been a well-established satellite product for over 40 years since Nimbus-7 (Herman et al. 1997).

2.2 Lagrangian particle dispersion model

To estimate the transport pathways of particles released from the biomass burning, the Lagrangian particle dispersion model FLEXPART version 10.3 was applied in this study (Pisso et al. 2019a). FLEXPART has been widely used for the analysis of pollutants' dispersion in South Asia region (Madala et al. 2016;

Corresponding author: Masayuki Takigawa, Institute of Arctic Climate and Environmental Research, Japan Agency for Marine-Earth Science and Technology, Kanazawa-Ku, Yokohama, Kanagawa 236-0001, Japan. E-mail: takigawa@jamstec.go.jp.

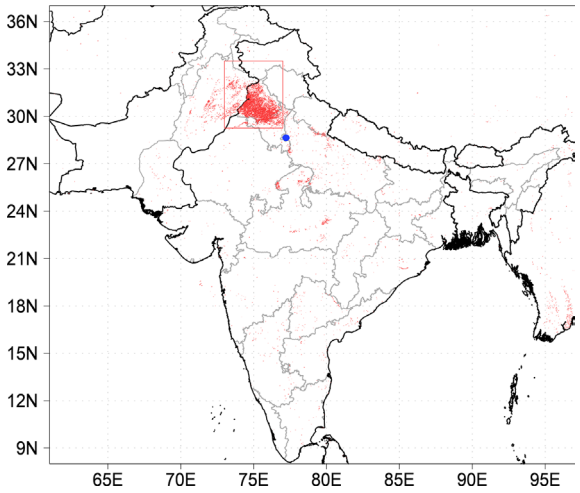

Fig. 1. The geographical location of Delhi NCR (blue circle). Hotspots of FIRMS (MODIS MCD14DL) from 1 October to 30 November 2019 are also shown as red dots. Gray lines denote the borders of states in India and Pakistan. Red-colored rectangle denotes the region including Punjab in India and Pakistan (29.25°N−33.5°N, 73°E−77°E).

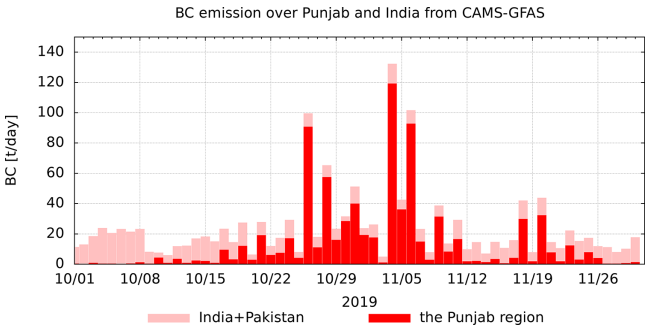

Fig. 2. Temporal variation of BC emission in CAMS-GFAS. Pink-colored bars denote the daily amount over India and Pakistan (8°N−37°N, 73°E−77°E), and red-colored bars denote over the Punjab region shown as the red rectangle in Fig. 1, respectively. Units are t(BC)/day.

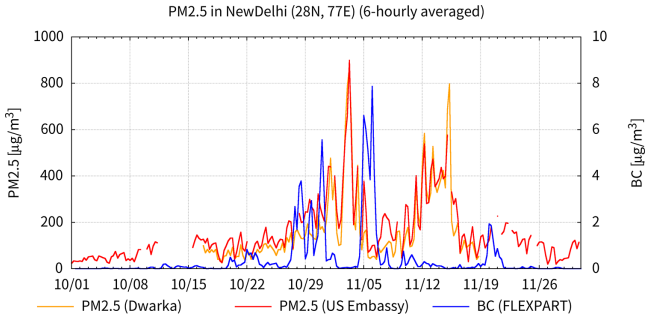

Fig. 3. Temporal variations of 6-hourly averaged PM2.5 concentration in New Delhi. Orange line denotes observation at Dwarka, and red line denotes at US Embassy, respectively. The concentration of BC emitted from biomass burning calculated by FLEXPART is also shown as blue lines (values are shown in the right axis). Units are μg/m^3.

Lal et al. 2014), and an updated version of physical-based wet deposition process for particles was implemented for in-cloud and below-cloud scavenging since version 10 (Grythe et al. 2017). A Gaussian-turbulence scheme was applied for the mixing within the boundary layer. The model was driven by the 0.25° NCEP operational global analysis ds083.3 (NCEP 2015). The time interval of analysis in NCEP analysis ds083.3 is 6 hours (00, 06, 12, and 18 UTC), and 3-hour forecasts from each analysis (03, 09, 15, and 21 UTC) were also used to improve the quality of temporal interpolation at each timestep of FLEXPART. As FLEXPART does not treat complex chemistry for the production of secondary organic carbon, BC was used to estimate the contribution of biomass burning emissions. BC is one of the constituents in PM2.5, and the fraction of BC to the total amount of primary PM2.5 emission from crop residue is estimated to be around 15% (Jain et al. 2014). The mean diameter of BC particles was modified from the original configuration in FLEXPART (from 0.4 μm to 0.25 μm) based on the observation over the IGP (Brooks et al. 2019).

2.3 Simulation for the 2019 Punjab fires

The simulation was conducted from 1 October to 30 November 2019 when extremely polluted events have been observed in Delhi. The procedure of the mean transit time calculation is described in Supplement 1. The emissions from biomass burning were taken from the ECMWF (European Centre for Medium-Range Weather Forecasts) CAMS (Copernicus Atmosphere Monitoring Service) -GFAS (Global Fire Assimilation System) (Rémy et al. 2017; Di Giuseppe et al. 2017; ECMWF 2019). The horizontal resolution of CAMS-GFAS is 0.1°, and the emissions were re-gridded into 0.5° to reduce the effect of missing emission around the hotspot. The release height was taken from the mass-weighted average of the injection height in the CAMS-GFAS emissions within the regridded 0.5° grid. If the injection height was zero in the CAMS-GFAS, the 'smoldering' emission was assumed to be released from the surface to 200 m above the ground. Day-to-day variation of BC emission in the CAMS-GFAS for the target region is shown in Fig. 2. A major fraction of the biomass burning BC in this region was emitted from the Punjab region.

3. Results

3.1 Effect of Punjab fires on the pollution in Delhi NCR

Temporal variations of 6-hourly averaged PM2.5 concentration in Delhi are shown in Fig. 3. Both instruments (BAM-1020 at the US embassy and the Panasonic-PM2.5 sensor at Dwarka) showed quite similar temporal variations with two large events during the target period, exceeding 900 μg/m^3 even for 6-hour average. The first high pollution event was from 28 October to 5 November, and the activity of biomass burning was also quite high during that period, except for 3 November, especially in the Punjab region (cf. Fig. 2). Almost no fire activity was detected on 3 November, and relatively lower fire activities on 1−2 November was noted by the MODIS sensor. The concentration of BC emitted from biomass burning calculated by FLEXPART is also shown in Fig. 3. It was the dry season of monsoon (typically from October to April), and the northwest wind was dominant over the IGP and the relative humidity was lower than 60% in most of the period.

Consequently, BC concentration in Delhi showed qualitatively comparable variations to that of BC emissions in Punjab with a time-lag of about 1 day. As the emission on 3 November and 12−15 November was quite small in CAMS-GFAS, the model could not reproduce the major peaks in the observations in Delhi on 3 and 12−15 November. Except for these "highly pollution" events, the modeled BC showed eventual increases which also appeared in the observed PM2.5 concentrations, especially around 29−31 October and 5 November.

3.2 Outflow of biomass burning plume across the Indo-Gangetic Plain

To track the movement of pollution across the IGP, UV Aerosol Index derived from S5P/TROPOMI was investigated over the source region (Punjab) and megacities in the downstream of monsoon (Delhi NCR and Kolkata). Region-wide average for the Punjab region (29.25°N−33.5°N, 73°E−77°E), the Delhi NCR region (28.3°N−28.9°N, 76.8°E−77.4°E), and Kolkata (22.2°N−22.7°N, 88.1°E−88.5°E) was calculated for each day, and the day-to-day variation for each region is shown in the upper panel

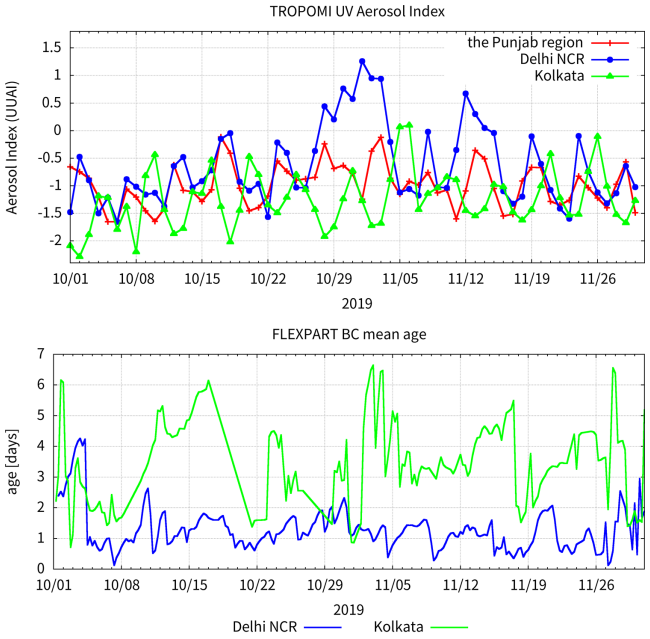

Fig. 4. (Upper panel) Temporal variations of ultraviolet Aerosol Index (UVAI) derived from the S5P/TROPOMI from 1 October to 30 November 2019. The region-wide average for the Punjab region (red line with crosses), the Delhi NCR region (blue line with circles; 28.3°N−28.9°N, 76.8°E−77.4°E), and Kolkata (green line with triangles; 22.2°N−22.7°N, 88.1°E−88.5°E) are shown. (Lower panel) Temporal variations of the mean transit time of biomass burning BC at Delhi NCR and Kolkata, estimated by FLEXPART. Units are days.

of Fig. 4. UVAI showed large positive values which indicate the existence of absorbing aerosols over Delhi from 28 October to 4 November (first event) and from 12 to 14 November (2nd event), and the temporal variation of UVAI was generally consistent with that of the observed surface PM2.5 concentration in Delhi (Fig. 3). Except for these large events, the variation in Delhi was generally corresponding with that of Punjab with a time-lag of about 1−2 days. It implies that the long-range transport from Punjab contributes to the pollution in Delhi in most days during the target period, but the large events might be caused as a mixture of local emission in Delhi and Punjab fires. This hypothesis is also supported by the greater UVAI values over Delhi than the source region of Punjab (28 October to 04 November; 11−15 November). The mean transit time estimated by FLEXPART is also shown in the lower panel of Fig. 4. It showed that the airmass with biomass burning emissions was transported from Punjab to Delhi within 2 days after the release. The carbon yield for the conversion from the non-methane organic gases (NMOG) to secondary organic carbon (SOA) was estimated to be about 40% after 2 days for biomass burning emissions (Lim et al. 2019) and produced SOA might also contribute to the increased UVAI in Delhi. Kolkata is located at the most downstream region in the IGP, about 1500 km away from Delhi. The temporal variation of UVAI in Kolkata was generally consistent with that of Delhi with a time lag of 2−3 days. The difference of mean transit time calculated by FLEXPART between Delhi and Kolkata was 1−4 days.

3.3 Day-to-Day movement of plumes from 30 October to 2 November 2019

Horizontal distribution of UVAI derived from S5P/TROPOMI from 30 October to 2 November is shown in Figs. 5a−5e. As the observation by S5P/TROPOMI is conducted at 13:30 LT (08 UTC for India), 6-hourly averaged modeled BC concentration from 06 UTC to 12 UTC (from 11:30 to 17:30 LT) near the surface is also shown as Figs. 5f−5j. The model treats BC emitted from the biomass burning only, but it generally succeeded to reproduce the day-to-day movement of plumes which was shown as UVAI showed large positive values. For example, the mean transit time of plume in Delhi showed 2−3 days on 30 October (Fig. 5f). It moved southeastward and reaches around Kolkata around 3 November, mixing with the local burning at the west side of Kolkata (dark blue lines on 2 and 3 November around Kolkata, which means young airmass (Figs. 5i and 5j). Southwestward transport could be seen on the west side of Delhi from 1 to 3 November (Figs. 5c−5e). As mentioned in Section 3.1, a high concentration of PM2.5 was observed in Delhi from 3 to 4 November.

Corresponding to that event, new plumes were existing over Punjab and the northern part of the Delhi NCR region in the observation (Fig. 5e). The model failed to reproduce eventual increase on 3 November around Delhi, but the model also showed the intrusion of young airmass (with a low concentration of BC) from Punjab to Delhi (Fig. 5j). It was also found that the polluted region was quite limited. By assuming the region of UVAI exceeding 2.0 to be a "highly-polluted" region, the size of the plume was estimated to be 20 × 100 km^2 on 1 November, and 30 × 40 km^2 on 3 November, respectively.

4. Discussion

To investigate the cause of the model's failure at the large event on 3 November, an additional calculation was conducted to estimate the origin of airmass. Based on the mean transit time estimation, 5-days' backward calculation of FLEXPART was conducted from Delhi at 06 UTC 3 November, when the observed concentration of PM2.5 was highest. The horizontal distribution of estimated residence time is shown in Fig. 6. As CAMS-GFAS uses the FRP of MODIS based on the temperature anomaly (Di Giuseppe et al. 2017), the cloudiness using MODIS Aqua (MYD 09GA) and the location of 1-km pixels which shows FRP is larger than 0 derived from MODIS is also shown in Fig. 6 (Freeborn et al. 2014). The number of hotspots was 831 in Punjab on 31 October, but there was no hotspot in MODIS Terra on 2 November, because hazy clouds covered Punjab and Delhi area since 1 November. The origin of airmass was estimated to be on the northwest side of Delhi including Punjab, but most of the footprint was covered by hazy clouds and a limited number of "clear" pixels were used for the estimation of hotspots. The relationship of the hotspot number and the cloud fraction over the Punjab region and the Delhi NCR region is shown in Fig. 7. Cloud fraction was quite large especially during the "most polluted" events in Delhi, such as the first event (3 November) and the second event (from 12 to 14 November). The number of hotspots rapidly decreased during these events, because more than 80% of the region was covered by the hazy cloud.

These results suggest that the estimation of day-to-day variation of the biomass burning emission is still challenging especially after the build-up of hazy clouds. In addition, MODIS tends to underestimate burned area in croplands because its resolution (500 m) is not enough especially for small (100 ha or smaller) fires (Zhu et al. 2017). There are several emission inventories for biomass burning, but most of them are based on MODIS temperature anomaly or burned area (Liu et al. 2020). Coupling of polar-orbiting satellites such as MODIS (500 m, 4 times in a day) and geostationary-orbiting satellites (e.g. ~4 km, every 5−15 minutes for GOES) might be useful to increase the number of observations over the target area (Li et al. 2019). Inverse model calculation with a ground-based observation network would be of importance to improve the spatio-temporal variation in a priori emissions (Lucas et al. 2017; Pisso et al. 2019b; Guo et al. 2018). The in situ PM2.5 measurement network should include high-density sites in the source regions, and cover the whole IGP extending towards the Bay of Bengal.

5. Conclusions

We have evaluated the possible pathways and the mean transit time of particles that were emitted from biomass burning, espe-

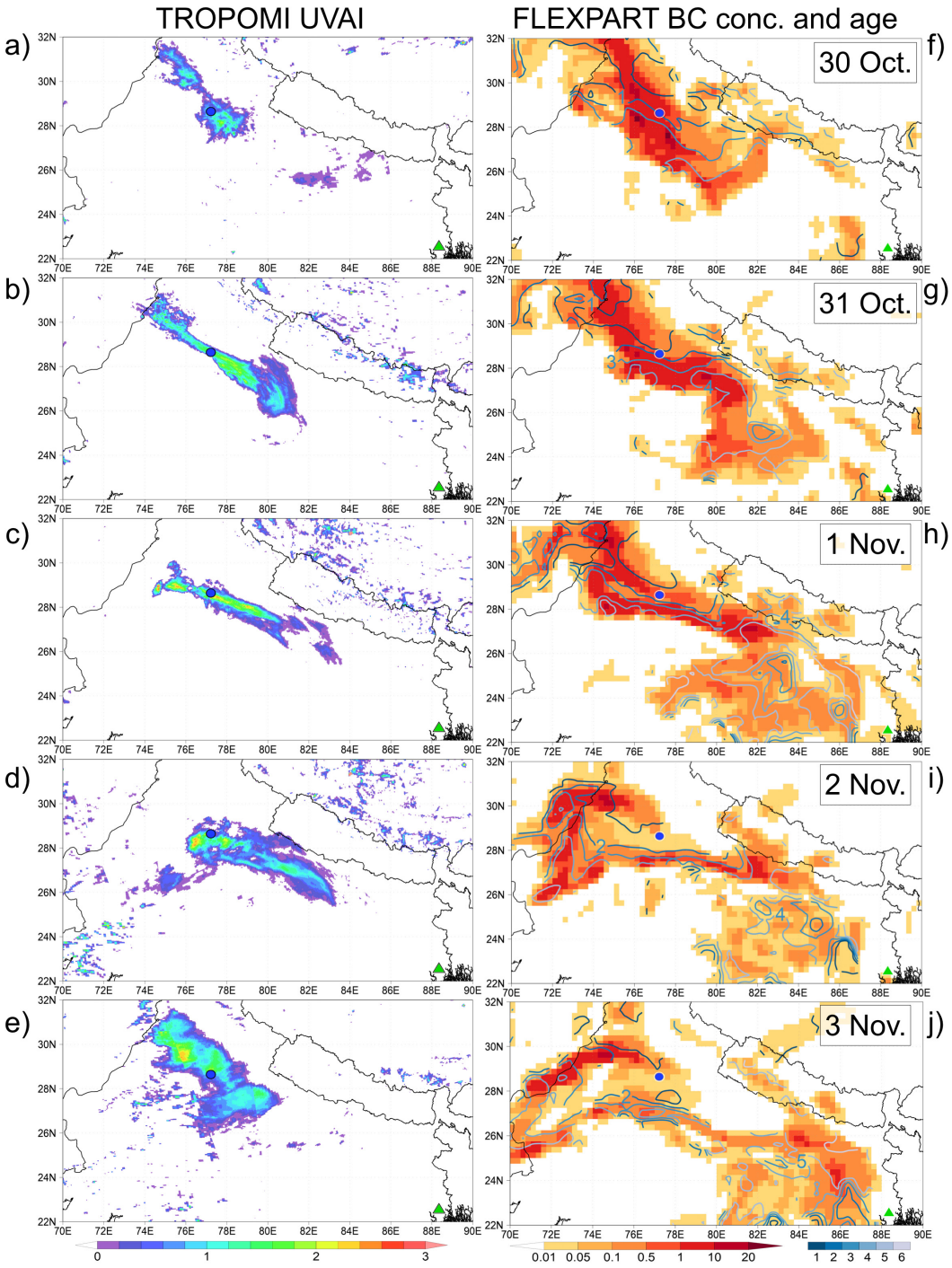

Fig. 5. a)–e): Horizontal distribution of UVAI derived from the S5P/TROPOMI from 29 October to 2 November 2019. f)–j) Biomass burning BC concentration near the surface calculated by FLEXPART. The unit is μg/m^3. Blue lines denote the mean transit time from the release. Blue circle and green triangle denote Delhi and Kolkata, respectively.

cially in the Punjab region to understand the time evolution of the high pollution episodes observed in Delhi in 2019. By using the FLEXPART forward calculation, the mean transit time to Delhi was estimated to be 1–2 days after the release. It was also found that the particles released from Punjab fire might travel across the IGP within a week during the dry monsoon season. The model failed to reproduce two distinguished polluted events in October–November 2019, but it was estimated that the airmass was transported from Punjab to Delhi on the days of the events by using the FLEXPART backward calculation. By analyzing the relationship between cloud fraction and FRP, it was suggested that the build-up of hazy clouds might reduce the possibility of the detection of hotspots from satellites. Calculation using models with much higher resolution (5 km or finer to reproduce the 30-km plume) such as WRF-FLEXPART might be also useful for evaluating the fine structure of plumes which was observed in S5P/TROPOMI (Brioude et al. 2013). For more detailed and quantitative analysis of PM2.5, it is needed to conduct calculations using three-dimensional chemical transport models such as WRF-Chem (Grell et al. 2005). Japan Meteorological Agency's Non-Hydrostatic Model (JMANHM) coupled with a chemical transport model (NHM-Chem) is another option, which provides a detailed aerosol rep-

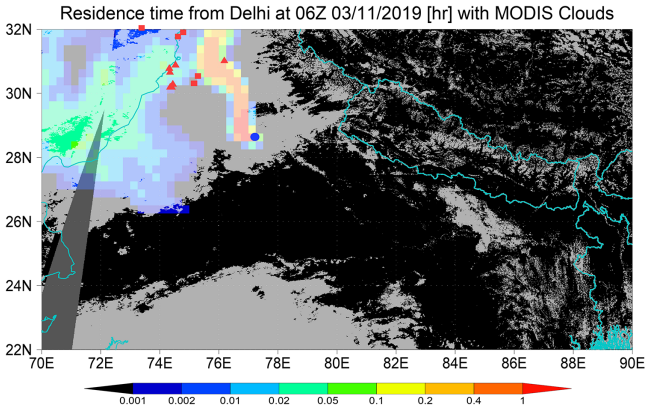

Fig. 6. Horizontal distribution of the residence time near the surface for the airmass at New Delhi at 06 UTC 3 November 2019 using 5-days' backward calculation of FLEXPART. Units are hours for each 0.25° × 0.25° grid. Light gray shade denotes the existence of clouds in MODIS Aqua on 2 November. Red squares and triangles denote hotspots (MODIS FRP > 0) on 2 and 3 November, respectively.

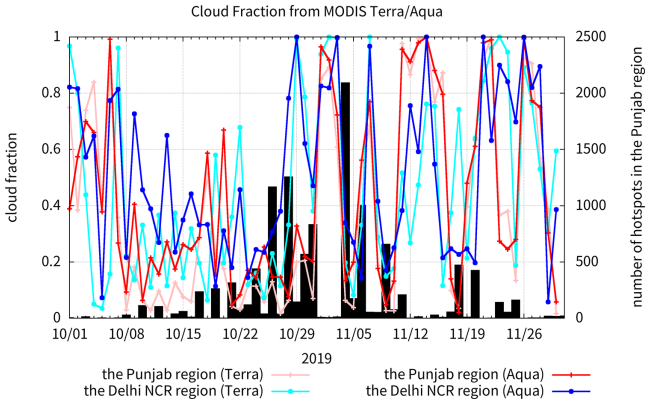

Fig. 7. Temporal variations of cloud fraction for MODIS Terra and Aqua derived from the daily surface reflectance from 1 October to 30 November 2019. Regions for the Punjab region (red and pink lines with crosses), the Delhi NCR region (blue and cyan lines with circles) are shown. Black bars denote the number of hotspots in the Punjab region derived from FRP of MODIS Aqua (MYD1406).

resentation method (Kajino et al. 2019). Large improvements in emission inventories and their refinements using the inversion of in situ observations are required for a better understanding of the regional air pollution for Delhi and the surrounding regions of the Indo-Gangetic Plain.

Acknowledgments

We appreciate the US Embassy for their PM2.5 observations. We also appreciate the developers of the FLEXPART model. The CAMS of ECMWF was used as a fire emission inventory, and the analysis has been done using CAMS Information and Copernicus Sentinel data downloaded in 2019. The analysis of TROPOMI, MODIS and FIRMS dataset is conducted using Google Earth Engine in November and December 2019. This research was supported by Research Institute for Humanity and Nature (RIHN: a constituent member of NIHU) Project No. 14200133 and partially supported by the Arctic Challenge for Sustainability (ArCS) Project of the Ministry of Education, Culture, Sports, Science and Technology (MEXT).

Edited by: O. Wild

Supplements

Supplement 1: The procedure for the calculation of the mean transit time.

References

Balakrishnan, K., and co-authors, 2019: The impact of air pollution on deaths, disease burden, and life expectancy across the states of India: The Global Burden of Disease Study 2017. *Lancet Planet Health*, **3**, e26−e39, doi:10.1016/S2542-5196(18)30261-4.

Brioude, J., and co-authors, 2013: The Lagrangian particle dispersion model FLEXPART-WRF version 3.1. *Geosci. Model Dev.*, **6**, 1889−1904, doi:10.5194/gmd-6-1889-2013.

Brooks, J., and co-authors, 2019: Black carbon physical and optical properties across northern India during pre-monsoon and monsoon seasons. *Atmos. Chem. Phys.*, **19**, 13079−13096, doi:10.5194/acp-19-13079-2019.

Chen, Y., O. Wild, L. Conibear, L. Ran, J. He, L. Wang, and Y. Wang, 2020: Local characteristics of and exposure to fine particulate matter (PM2.5) in four indian megacities. *Atmos. Environ.: X*, **5**, 100052, doi:10.1016/j.aeaoa.2019.100052.

Cusworth, D. H., L. J. Mickley, M. P. Sulprizio, T. Liu, M. E. Marlier, R. S. DeFries, S. K. Guttikunda, and P. Gupta, 2018: Quantifying the influence of agricultural fires in northwest India on urban air pollution in Delhi, India. *Environ. Res. Lett.*, **13**, 044018, doi:10.1088/1748-9326/aab303.

Di Giuseppe, F., S. Rémy, F. Pappenberger, and F. Wetterhall, 2017: Combining fire radiative power observations with the fire weather index improves the estimation of fire emissions. *Atmos. Chem. Phys.*, doi:10.5194/acp-2017-790.

ECMWF, 2019: CAMS Global Fire Assimilation System. Accessed 4 November 2019, https://apps.ecmwf.int/datasets/data/cams-gfas/.

Freeborn, P. H., M. J. Wooster, D. P. Roy, and M. A. Cochrane, 2014: Quantification of MODIS fire radiative power (FRP) measurement uncertainty for use in satellite-based active fire characterization and biomass burning estimation. *Geophys. Res. Lett.*, **41**, 1988−1994, doi:10.1002/2013GL059086.

Grell, G. A., S. E. Peckham, R. Schmitz, S. A. McKeen, G. Frost, W. C. Skamarock, and B. Eder, 2005: Fully coupled "online" chemistry within the WRF model. *Atmos. Environ.*, **39**, 6957−6975, doi:10.1016/j.atmosenv.2005.04.027.

Grythe, H., N. I. Kristiansen, C. D. Groot Zwaaftink, S. Eckhardt, J. Ström, P. Tunved, R. Krejci, and A. Stohl, 2017: A new aerosol wet removal scheme for the Lagrangian particle model FLEXPART v10. *Geosci. Model Dev.*, **10**, 1447−1466, doi:10.5194/gmd-10-1447-2017.

Guo, L., and co-authors, 2018: Improving PM2.5 Forecasting and Emission Estimation Based on the Bayesian Optimization Method and the Coupled FLEXPART-WRF Model. *Atmosphere*, **9**, 428, doi:10.3390/atmos9110428.

Guttikunda, S. K., R. Goel, and P. Pant, 2014: Nature of air pollution, emission sources, and management in the Indian cities. *Atmos. Environ.*, **95**, 501−510, doi:10.1016/j.atmosenv.2014.07.006.

Hall, T. M., and R. A. Plumb, 1994: Age as a diagnostic of stratospheric transport. *J. Geophys. Res.*, **99**, 1059, doi:10.1029/93JD03192.

Herman, J. R., P. K. Bhartia, O. Torres, C. Hsu, C. Seftor, and E. Celarier, 1997: Global distribution of UV-absorbing aerosols from Nimbus 7/TOMS data. *J. Geophys. Res.*, **102**, 16911−16922, doi:10.1029/96JD03680.

Jain, N., A. Bhatia, and H. Pathak, 2014: Emission of Air Pollutants from Crop Residue Burning in India. *Aerosol Air Qual. Res.*, **14**, 422−430, doi:10.4209/aaqr.2013.01.0031.

Jethva, H., D. Chand, O. Torres, P. Gupta, A. Lyapustin, and F. Patadia, 2018: Agricultural burning and air quality over Northern India: A synergistic analysis using NASA's A-train

satellite data and ground measurements. *Aerosol Air Qual. Res.*, **18**, 1756−1773, doi:10.4209/aaqr.2017.12.0583.

Kajino, M., and co-authors, 2019: NHM-chem, the Japan Meteorological Agency's regional meteorology – Chemistry model: Model evaluations toward the consistent predictions of the chemical, physical, and optical properties of aerosols. *J. Meteor. Soc. Japan*, Ser. II, **97**, 337−374, doi:10.2151/jmsj.2019-020.

Kanawade, V. P., A. K. Srivastava, K. Ram, E. Asmi, V. Vakkari, V. K. Soni, V. Varaprasad, and C. Sarangi, 2019: What caused severe air pollution episode of November 2016 in New Delhi? *Atmos. Environ.*, **222**, 117125, doi:10.1016/j.atmosenv.2019.117125.

Lal, S., S. Venkataramani, N. Chandra, O. R. Cooper, J. Brioude, and M. Naja, 2014: Transport effects on the vertical distribution of tropospheric ozone over western India: Transport effects on ozone distribution. *J. Geophys. Res. D: Atmos.*, **119**, 10012−10026, doi:10.1002/2014JD021854.

Li, F., X. Zhang, D. P. Roy, and S. Kondragunta, 2019: Estimation of biomass-burning emissions by fusing the fire radiative power retrievals from polar-orbiting and geostationary satellites across the conterminous United States. *Atmos. Environ.*, **211**, 274−287, doi:10.1016/j.atmosenv.2019.05.017.

Lim, C. Y., and co-authors, 2019: Secondary organic aerosol formation from the laboratory oxidation of biomass burning emissions. *Atmos. Chem. Phys.*, **19**, 12797−12809, doi:10.5194/acp-19-12797-2019.

Liu, T., L. J. Mickley, M. E. Marlier, R. S. DeFries, M. F. Khan, M. T. Latif, and A. Karambelas, 2020: Diagnosing spatial biases and uncertainties in global fire emissions inventories: Indonesia as regional case study. *Remote Sens. Environ.*, **237**, 111557, doi:10.1016/j.rse.2019.111557.

Lucas, D. D., M. Simpson, P. Cameron-Smith, and R. L. Baskett, 2017: Bayesian inverse modeling of the atmospheric transport and emissions of a controlled tracer release from a nuclear power plant. *Atmos. Chem. Phys.*, **17**, 13521−13543, doi:10.5194/acp-17-13521-2017.

Madala, S., K. B. R. R. Hari Prasad, C. V. Srinivas, and A. N. V. Satyanarayana, 2016: Air quality simulation of NOX over the tropical coastal city Chennai in southern India with FLEXPART-WRF. *Atmos. Environ.*, **128**, 65−81, doi:10.1016/j.atmosenv.2015.12.052.

Mukherjee, T., A. Asutosh, S. K. Pandey, L. Yang, P. P. Gogoi, A. Panwar, and V. Vinoj, 2018: Increasing potential for air pollution over megacity New Delhi: A study based on 2016 Diwali Episode. *Aerosol Air Qual. Res.*, **18**, 2510−2518, doi:10.4209/aaqr.2017.11.0440.

Nakayama, T., Y. Matsumi, K. Kawahito, and Y. Watabe, 2018: Development and evaluation of a palm-sized optical PM2.5 sensor. *Aerosol Sci. Technol.*, **52**, 2−12, doi:10.1080/02786826.2017.1375078.

NASA, 2019: MODIS/Aqua+Terra thermal anomalies/fire locations 1km FIRMS V006 NRT. *MCD14DL*, Accessed 6 January 2020, https://doi.org/10.5067/FIRMS/MODIS/MCD14DL.NRT.006.

NCEP, 2015: NCEP GDAS/FNL 0.25 degree global tropospheric analyses and forecast grids. Accessed 6 January 2020, https://doi.org/10.5065/D65Q4T4Z.

Pisso, I., and co-authors, 2019a: The Lagrangian particle dispersion model FLEXPART version 10.3. *Atmos. Sci.*, doi:10.5194/gmd-2018-333-RC1.

Pisso, I., P. Patra, M. Takigawa, T. Machida, H. Matsueda, and Y. Sawa, 2019b: Assessing Lagrangian inverse modelling of urban anthropogenic CO2 fluxes using in situ aircraft and ground-based measurements in the Tokyo area. *Carbon Balance Manag.*, **14**, 6, doi:10.1186/s13021-019-0118-8.

Rémy, S., and co-authors, 2017: Two global data sets of daily fire emission injection heights since 2003. *Atmos. Chem. Phys.*, **17**, 2921−2942, doi:10.5194/acp-17-2921-2017.

Saraswat, A., J. S. Apte, M. Kandlikar, M. Brauer, S. B. Henderson, and J. D. Marshall, 2013: Spatiotemporal land use regression models of fine, ultrafine, and black carbon particulate matter in New Delhi, India. *Environ. Sci. Technol.*, **47**, 12903−12911, doi:10.1021/es401489h.

Sawlani, R., R. Agnihotri, C. Sharma, P. K. Patra, A. P. Dimri, K. Ram, and R. L. Verma, 2019: The severe Delhi SMOG of 2016: A case of delayed crop residue burning, coincident firecracker emissions, and atypical meteorology. *Atmos. Pollut. Res.*, **10**, 868−879, doi:10.1016/j.apr.2018.12.015.

Sharma, A. K., P. Baliyan, and P. Kumar, 2018: Air pollution and public health: The challenges for Delhi, India. *Rev. Environ. Health*, **33**, 77−86, doi:10.1515/reveh-2017-0032.

Stein Zweers, D. C., 2018: TROPOMI ATBD of the UV aerosol index. Accessed 27 December 2019, https://sentinels.copernicus.eu/documents/247904/2476257/Sentinel-5P-TROPOMI-ATBD-UV-Aerosol-Index.

U. S. Embassy in India, 2019: Air quality data. Accessed 19 November 2019, https://in.usembassy.gov/embassy-consulates/new-delhi/air-quality-data/.

US EPA, 2016: List of designated reference and equivalent methods. Accessed 26 December 2019, https://www3.epa.gov/ttnamti1/files/ambient/criteria/AMTIC%20List%20Dec%202016-2.pdf.

WHO, 2016: *Ambient Air Pollution: A Global Assessment of Exposure and Burden of Disease*. Department of Public Health, Environmental and Of Health, Social Determinants, World Health Organization, 131 pp.

Zhu, C., H. Kobayashi, Y. Kanaya, and M. Saito, 2017: Size-dependent validation of MODIS MCD64A1 burned area over six vegetation types in boreal Eurasia: Large underestimation in croplands. *Sci. Rep.*, **7**, 4181, doi:10.1038/s41598-017-03739-0.

Manuscript received 7 January 2020, *accepted 22 March 2020*
SOLA: *https://www.jstage.jst.go.jp/browse/sola/*